Measured Hot Spot Directional Signatures of Agricultural Crops during DAISEX'99 using POLDER data

F. Camacho-de Coca[1], M. Leroy[2], J.P. Gastellu-Etchegorry[2] and F.J. García-Haro[1]
[1]*Department of Thermodynamics, University of Valencia.*
C/Dr. Moliner, 50. 46100 Burjassot. Valencia, Spain.
[2] *CESBIO, UMR CNES-CNRS-UPS*
18,av. e. belin, 31055. Toulouse, France.
fernando.camacho@uv.es, marc.leroy@medias.cnes.fr

ABSTRACT- *In this paper, we have investigated several hot spot directional signatures of different agricultural crops measured with the POLDER instrument during the DAISEX'99 campaign. This instrument provides us with a directional resolution of about 0.3º in phase angle and a spatial resolution of 20 m. The hot spot signature is retrieved with the assumption of spatial homogeneity of the target. The spectral dependence of the hot spot has been investigated in four channels (443, 550, 670 and 800 nm). The hot spot directional signature has been fitted to a function of the phase angle as predicted by the radiative transfer theory within the leaf canopies. The retrieved parameters (half width and amplitude) show different findings. The half width values have ranged between 1 and 2 degrees, being quite independent of the canopy cover type. The amplitude values have shown results according with the expected reflectance of the scatters. The estimated leaf reflectance values at noon were typically 0.4 in the near infrared region for all vegetated unit. The spectral leaf reflectance is consistent and shows the potential of the hot spot measurements to retrieve the leaf biochemical content.*

1 INTRODUCTION

When the angle between the sun and view directions (phase angle, ξ) tends to zero the reflected radiance of a surface rises sharply up to its maximum value, exactly at zero phase angle. Seelinger interpreted correctly this effect observing Saturn's rings (Seelinger 1887). In optical remote sensing, this effect is known as the hot spot and it constitutes a fine BRDF signature of the Earth's surfaces. It was initially observed in aerial photography as a bright area around the shadow of the plane. From the first moment, the hot spot was recognized as possible structural identifier of the vegetation canopies (Gerstl and Simmer 1986).

From Seelinger up to now, the shadow-hiding mechanism (Hapke et al. 1996, Hapke 1993) has been the physical process accepted to explain the hot spot effect. This mechanism takes place when the size of scatters is large compared with the wavelength and, thus, well-defined shadows appear. These shadows are visible at large phase angle but close to zero phase angle they are hiding by the objects (leaves, soil particles) that cast them. Hence, close to the backscattering the reflectance is manifestly enhanced. In addition, when the size of scatters is lower or approximately equal to the wavelength, the shadow-hiding mechanism cannot describe properly the hot spot effect. A different mechanism known as coherent-backscatter or weak photon localization has been then identified as responsible of the hot spot. The coherent-backscatter explains the hot spot as a constructive interference phenomenon (Barabanenkov et al. 1991). The half width of the coherent-backscatter peak increases linearly with the wavelength, whereas in the shadow-hiding theory the half width of the hot spot is expected to be independent of wavelength. Furthermore, single scattering does not contribute to coherent-backscattering, which depends on multiply scattered light, whereas the shadow-hiding is important only for once scattered radiation.

Many hot spot models, mostly accounted for by the shading mechanism, have been developed in order to incorporate the hot spot to the leaf canopy BRDF models. A review of hot spot modeling can be found in Qin and Goel (1995). These models point out the interest in the hot spot measurements from remote sensing applications. Since the half width of the hot spot is proportional to the photon mean free path, it should be dependent of structural parameters such us leaf area index (LAI), leaf dimension (D) or canopy height (H). Therefore, the hot spot could have utility as a land cover classifier. Moreover, the amplitude of the hot spot gives access to the reflectance of the foliage elements or soil grains (Bréon et al. 2002).

The possibility to obtain the hot spot directional signature from remote sensing platforms has been demonstrated in the literature (Bréon et al. 1997). The first hot spot data set of major biomes from space have already been produced using the POLarization and Directionality of Earth Reflectance (POLDER) instrument onboard the ADvanced Earth Observing System (ADEOS) (Bréon et al. 2002). The analysis of this data set shows a lower variability in the hot spot

half widths than the expected from the theoretical approaches (Qin and Goel, 1995), whereas the amplitude of the hot spot presents proportional values to the leaf reflectance.

The measurement and analysis of the hot spot effect was one of the priorities during the Digital Airborne Spectrometer Experiment (DAISEX) campaigns of the ESA (ESA 2001). In the 1999 campaign, the POLDER and the Hyperspectral MAPping (HyMAP) instruments recorded satisfactorily the hot spot directional signatures of different agricultural crops. In this paper, we present the results of the hot spot directional signatures measured using POLDER imagery. Our main objective is to analyze the potential and limits of the hot spot signature to retrieve canopy biophysical information.

2. EXPERIMENT DESCRIPTION

2.1. Test Site

The experiment site is a 3 km by 3 km area centered at 39º 3' N, 2º 5' W, which is located 28 km from Albacete (Spain), close to the Barrax town. This area was selected by ESA for the DAISEX campaigns during 1998, 1999 and 2000 (ESA 2001). The POLDER instrument flew in the 1999 campaign**.** A supervised classification of the area was made based on field information. During that summer, the dominant cultivation in the area was approximately 53% dry land (29% barley, 24% fallow) and 42% irrigated land (15% corn, 11% alfalfa, 8% wheat; 2% legumes, 2% sugar beet, and 4% others) with a 5% of unclassified data.

2.2 Airborne POLDER data

In the DAISEX campaign, the spectral filters of the POLDER instrument were centered at 443, 500, 550, 590, 670, 700, 720, 800, and 864 nm wavelength. The POLDER field-of-view (FOV) was along track and cross track of ±43º and ±51º respectively. This resulted in a ground FOV of 7.4×5.6 km^2 for the typical flight altitude of 3000 m. At this flight altitude the spatial resolution was 20 m (Leroy et al. 2001).

Four flights with the ARAT plane carrying POLDER and LEANDRE instruments were performed in the 1999 campaign. They correspond to 3rd June at noon (from 11:29 to 12:31 UT), 4th June in the morning (from 07:16 to 08:15 UT) and in the afternoon (from 13:57 to 15:01 UT), and 5th June in the morning (from 06:57 to 08:02 UT). In each flight the POLDER instrument records around 140 spectral images, which constitutes a POLDER sequence. One image is acquired within 3 seconds, and the acquisition is repeated every 10 seconds, with an overlap between consecutives images. Thus, in a sequence, every pixel is observed with different viewing directions, typically between 30-60 covering a wide range of the directional space. The POLDER reflectance images were calibrated, geo-coded and corrected for atmospheric effects as it is specified in Leroy et al (2001).

3. METHODOLOGY

The methodology followed is that of Bréon et al (2002), which is mainly based on an original measurement principle to retrieve hot spot at a fine spatial resolution from POLDER imagery. This methodology is briefly described below.

3.1. Measurement principle

In a sequence of POLDER images, the viewing geometry for a pixel given changes between 5-10º degrees in consecutive snapshots covering the full directional range. This is a suitable directional resolution to reconstruct the BRDF of the surfaces. However, for a proper description of the reflectance enhancement at the backscattering, a finer directional resolution is needed and, consequently, a new measurement principle should be considered. This measurement principle is based on the assumption of spatial homogeneity of the target. If this assumption is verified then the variability in the measured radiance with the viewing angle may be considered as a directional signature. Thereby, a spatial heterogeneity correction should be done in order to reduce spurious contribution to the reflectance variability with the viewing geometry. Once we identify a hot spot belonging to a homogeneous area, we measure the reflectance corresponding to a region centered in the hot spot pixel. The size of this region will be determined by the spatial resolution and the typical size of the samples. In this work, the maximum size of the hot spot region is 7×7 pixels (approximately 140×140 m^2). In this area, the phase angle changes typically 0.3º per pixel. Thanks to the multi-angular POLDER data, we can use different snapshots in order to increase the directional coverage. This method was satisfactorily tested over an Australian site and later applied on a global scale using POLDER data (Bréon et al. 2002).

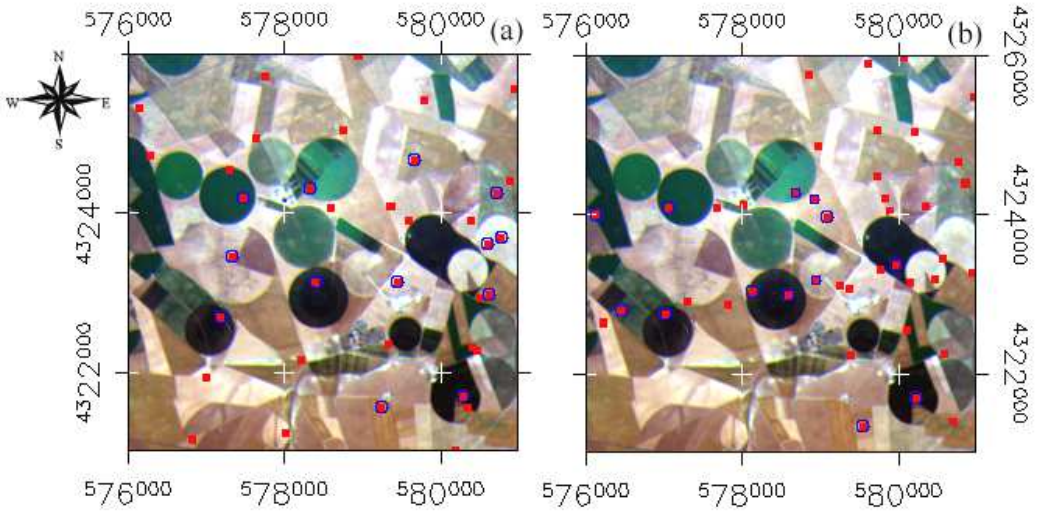

Figure 1. Location of the hot spots (band 5) in the study area: a) Noon, b) Afternoon.

3.2. Data processing

We have only processed the POLDER atmospherically corrected data acquired at noon and in the afternoon. In the other two flights, the POLDER FOV is lower than the sun zenith angle and, thereby, the hot spot condition is not satisfied by any pixel in the image. In order to undertake a spectral analysis of the hot spot we have selected four bands: 443 nm, 550 nm, 670 nm and 800 nm. The blue band serves to identify an aerosol contribution to the backscattering peak. First, we have identified for each image the pixel satisfying the hot spot condition, locating 79 hot spots from 205 useful snapshots. Figure 1 shows the exact location of the hot spots in band 5 (670 nm). Afterwards, only 27 hot spots belonging to homogeneous fields and far enough from the crop boundary were identified (blue circles in the figure 1). In fact, the hot spot location moves around 250 m from the first to the last band, which is roughly a half of the field length. It hampers the spectral analysis of the hot spot because some spectral channels will be missing. For the final selection of the spectral hot spots, we have obtained the nadir reflectance in a 7x7 pixels window centered at backscattering. A threshold of 10% in the variability coefficient (mean value/standard deviation) was found to give satisfactory results to filter out heterogeneous samples. Finally, 24 hot spot were selected (12 at noon + 12 in the afternoon) but the four spectral channels have been only considered in 12 cases (7+5) (see table 1).

For increasing the directional coverage of the hot spot directional signature, we have made use of additional images of the corresponding POLDER sequence. In order to minimize the fluctuations induced by the apparent solar movement, we have used only those sequences where the change in the sun zenith angle is lower than 0.5º at noon and lower than 1.5º in the afternoon. A simple spatial heterogeneity correction has been made using patches of data far away from the backscattering. The deviation from the mean reflectance was considered as a bias that was subsequently subtracted from the hot spot directional signature.

The hot spots belong to different agricultural cover types, from bare soil to the densest alfalfa crop. Then, the next step was the classification of the located hot spots (see table 1). The number of hot spots (HS) is expressed as the sum of the two flights.

Table 1. Structural parameters and number of hot spots (Noon + Afternoon) of the different selected samples.

Samples	Acronym	HS	Height (m)	LAI	FVC* (%)
Corn	C	3+1	0,12-0,2	0,26±0,11	25
Wheat	W	3+5	0,7-0,85	-	95
Barley	B	3+3	0,55-0,65	3,2±0,4	90
Alfalfa	A	1+1	0,6-0,7	2,5±0,5	100
Alfalfa cut	Ac	0+1	-	-	75
Legumes	L	0+1	-	-	100
No classified	N.C.	1+0	-	-	-
Soil	S	1+0	-	-	0

The available field data show similarities in height and LAI for the developed alfalfa, wheat and barley crops. The fraction of vegetation coverage (FVC) was derived from HyMAP imagery using a variable and multiple endmember spectral mixture analysis (VMESMA) procedure (García-Haro et al. 2002).

3.3. Theoretical approach

The theoretical approach followed to retrieve biophysical information from the hot spot signature is that of Bréon et al (2002). This model assumes geometrical-optical principles to derive the overlap function, S, based on the model of Jupp and Strahler (1991). They define this function as the ratio between the illuminated shadow and the view shadow to the nadir projection area. They used then the Boolean set theory for developing a more general algorithm of the hot spot in continuous canopies with horizontal distributed leaves. Bréon et al (2002) assume randomly distributed leaves (uniform angular distribution). In this case, the mean projection of the leaf surfaces along a particular direction defined by θ is constant, ½. The hot spot is explained as a correlation between the downward and upward transmissions. Hence, at a level z, the apparent position of the leaves is correlated regarding the inward and outward radiance paths. Consequently, the leaf area density considered is not $u_L(t)\delta t$ but rather $u_L(t)[1-S(d/D)/2]\delta t$, where u_L is the leaf area density at a level t, D is the typical leaf dimension, d is the decorrelation length and S is the overlap function. In the case of uniform oriented leaves, the decorrelation length is related to the phase angle (ξ) rather than to the more common $\Delta(\theta_s,\theta_v,\varphi)$ function. The decorrelation length is then written as (see formal demonstration in Bréon et al 2002):

$$d = \frac{2(z-t)}{\mu_s + \mu_v} \cdot \xi \qquad (1)$$

where $\mu_{s,v}=\cos\theta_{s,v}$

The expression for the upward and downward transmission is then used to derive the single scattering reflectance R_s for thick canopies with a negligible soil contribution. The radiative transfer modeling indicates that the reflectance can be fitted accurately using the following expression.

$$R = \frac{\Delta R_{HS}}{1 + \xi / \xi_0} + b\xi + c \qquad (2)$$

ΔR_{HS} is the amplitude of the hot spot, which is given by the difference of the modeled reflectance when consider the hot spot effect (S=1) and without consider it (S=0).

$$\Delta R_{HS} = \frac{1}{2} R_s \big)_{\xi=0} = \frac{\rho_{leaf}}{3\mu_s} \qquad (3)$$

where ρ_{leaf} is the leaf reflectance.

And ξ_0 is the half width at half maximum:

$$\xi_0 = \frac{LD}{6.4H} \qquad (4)$$

Hence, we can fit the measured data to the function expressed in equation 1 to derive the amplitude and the half width of the hot spot. The half width is related to the ratio between LAI, leaf size and height of the cover, whilst the amplitude is related to the leaf reflectance.

4. RESULTS AND DISCUSSION

Figure 2 shows a selection of the hot spot directional signatures obtained from the POLDER sequence. A window of 7×7 pixels (140×140 m^2) was used for every patch view, each one corresponding to a different image. The data is plotted as a function of the signed phase angle. This takes a positive value if the corrected view angle ($\theta_v \cos\varphi$) is larger than the solar zenith angle and vice versa. We can observe that from approximately –40º to -10º the reflectance increase linearly. This trend is associated to the macro-structure of the sample and, thus, can be connected to the surface scattering process. Beyond –40º the linear trend fails and the reflectance increase because of the so-called gap effect, mostly for vertical oriented canopies in presence of the multiple scattered radiation (e.g. figure 2g and 2h). Close to the backscattering the reflectance increases sharply since the phase angle tends to zero due to the hot spot effect. This trend is now associated to a different physical mechanism linked to the volume scattering process, *i.e.* the joint probabilities of transmission of penetrating and reflected radiation within the canopy. Thereby, the term of hot spot should be reserved only to this fine resolution peak. Figure 2 shows also the theoretical hotspot signature as predicted by equation 2. We can observe a good fit of the function in the interval from –40º to 5º phase angle. Results have also shown that this function provides a lower RMS error than the more common exponential function (Kuusk, 1985). Moreover, for the fitting approach considered, it gives narrower and more realistic half widths, especially in the afternoon flight where the directional signature presents a lower number of data. These results are in agreement with the fact that the exponential function overestimates the hot spot width with relation to other approaches (Qin and Goel, 1995), mainly because the exponential function does not vanish even when there is not overlap. In figure 2 we can see that the hot spot effect appears independently of the canopy cover type. The hot spot directional signatures show a similar behavior for the soil, the class with lowest cover (corn), and the senescent barley. The optical properties of these classes change linearly with the wavelength. In contrast, the samples with a high amount of photosynthetically active vegetation, such as the wheat

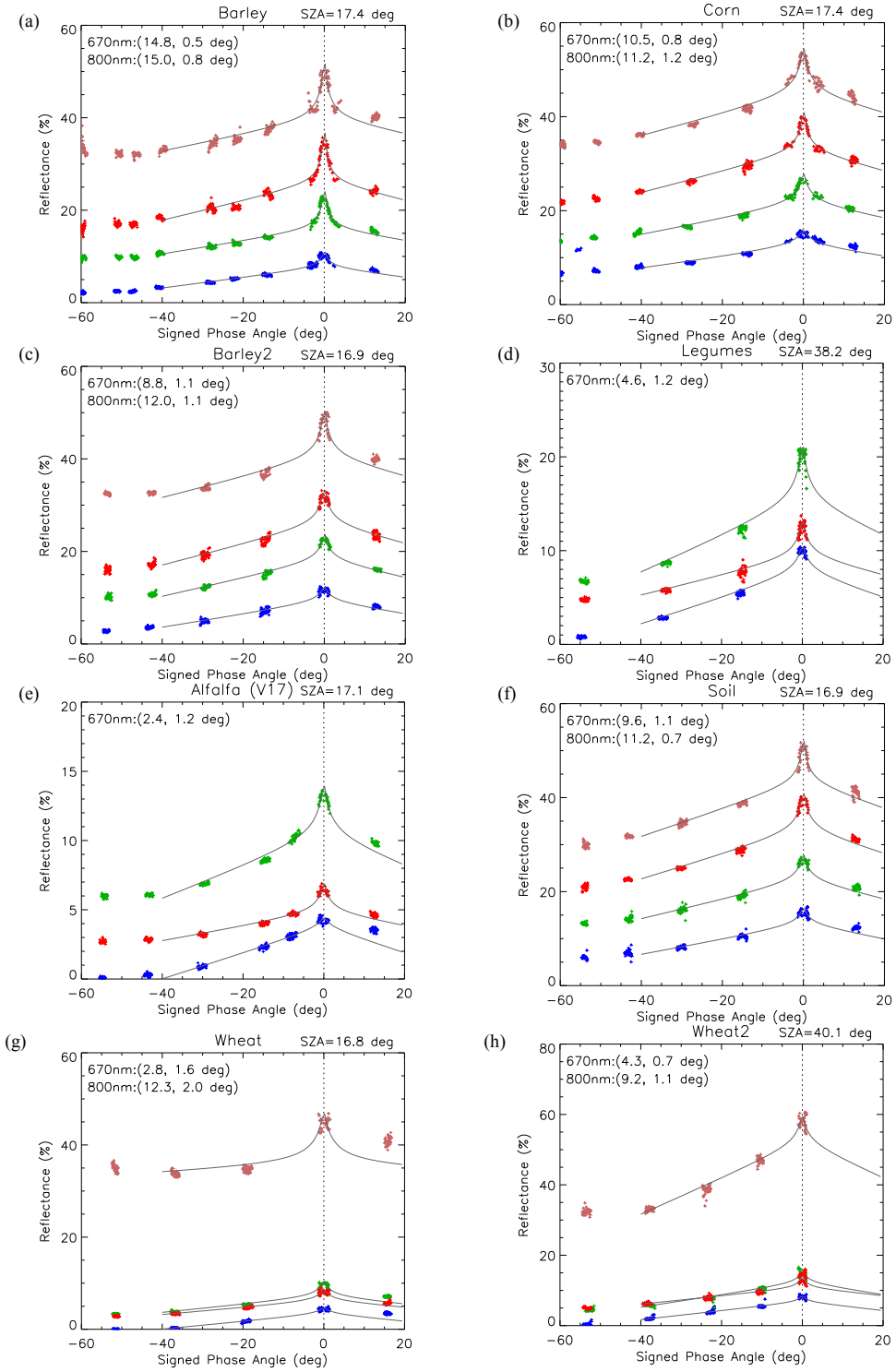

Figure 2. Hot Spot directional signatures as a function of the signed phase angle (negative when $\theta_v \cos\varphi < \theta_s$) measured under different sun zenith angle (SZA). The line shows the fit of the data using the function of equation 2. On the top left side is written the amplitude and the half width at 670 and 800 nm.

cover, present greater differences between the visible and NIR signatures. On the top left side of the graphs, we have showed the retrieved values for the amplitude and the half width at 670 nm and 800 nm. The barley cover is shown twice (figures 2a and 2c). In figure 2a, the hot spot peak has been characterized using two images whilst in figure 2c only one image has been used. The use of two patches close to the backscattering results in a more accurate representation of the hot spot effect and, consequently, retrieved parameters offer a higher confidence. The differences are quite important in both amplitude and half width. This is no surprising because the higher the sampling in the hot spot domain, the better the likely accuracy of retrieved parameters. For the wheat sample the two graphs corresponds to the two different flights. In this case, the number of patches considered in the fit is also different. The results show also large differences in both amplitude, affected by the sun position, and half width. In this case, we should note a higher spatial variability that results in a worse fit around the hot spot.

For improving the stability of the solutions, the fit was made in a two-step process. First, the linear part was fitted to the data existing between –10º and –40º to derive the linear coefficients b and c. Then the equation was fit between a phase angle limit of –20º and +5º to derive the amplitude and the half width. The root mean square (RMS) error was calculated to evaluate the fit quality around the hot spot (± 5º). In addition, the amplitude to RMS ratio has been used to evaluate the signal-to-noise ratio of the measured hot spot signatures. The values of the relative RMS are typically 2-4% in the noon flight and 4-7% in the afternoon. It shows the best quality of the hot spot fit in the noon flight images. For spectral channels, the blue band shows the worst fit in relative terms, whereas the near infrared band shows the lowest values. The signal-to noise ratio was higher at 550 nm, with typical values of 14 at noon and 10 in the afternoon, whereas the worst ratio values (<10) were found at 443. In general, the signal-to-noise ratio shows slightly higher values at 670 nm than at 800 nm. Neither RMS nor signal-to-noise ratio present significant differences regarding the canopy cover type.

To assess the stability of retrieved parameters, a sensitivity analysis has been conducted by combining 3 different window sizes (25, 36, 49 pixels) with 3 different phase angle limits L={-15º, -20º, -25º}. This analysis provides us with the confidence interval of the estimates. In general, the retrieved amplitude increases and the half width decreases slightly with the window size, i.e. at increasing the number of points depicting the hot spot. Concerning the phase angle limits considered in this assessment, the retrieved parameters are quite insensitive showing differences on the order of 0.1 in both amplitude and half width.

Figure 3 shows the estimated hot spot half widths, which mostly range between 1º and 2º. The samples have been ordered from low to high vegetation coverage; a different number with the same label indicates different parcel, whilst C and C´ (W and W´) refers to the same parcel. We can observe the lack of a regular tendency with the canopy cover type, including bare soil and densest vegetated surfaces such as alfalfa or wheat. The results indicate that at this spatial and directional resolution the half width presents a lower variability than that predicted by the above model. This finding has been previously reported in Bréon et al (2002) over the major IGPB land cover types. Therefore, it seems to be quite difficult to interpret the hot spot half width in terms of structural parameters of the canopy cover. In fact, the hot spot formation should be a quite complex problem since vegetation canopies present a detailed architecture with different elements such us leaves, buds and also spikes in developed cereal crops, with a particular level of aggregation (clumping) and interstices trough which light can penetrate (Roujean 2000). However, most of the hot spot modeling has been accounted for by using the leaf or the crown as the basic unit to compute the mutual shadowing, which is a strong simplification (Qin and Goel 1995). In addition, the distribution of the data points in the hot spot region seems to be insufficient for

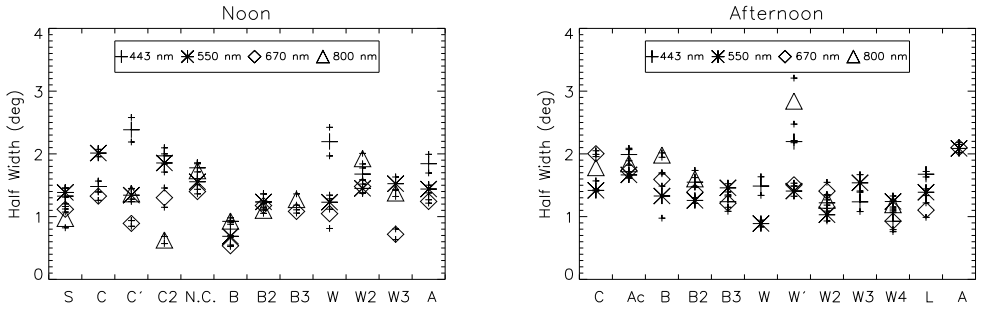

Figure 3. Retrieved hot spot half width in the noon and in the afternoon flights (acronyms appears in table 1).

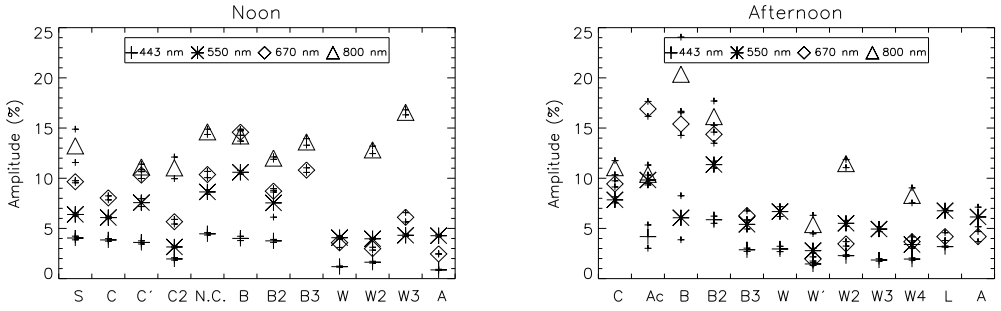

Figure 4. Retrieved hot spot amplitude in the noon and in the afternoon flights (acronyms appears in table 1).

determining accurately the amplitude and half width of the hot spot peak. We have more confident in the results with a better sampling.

Concerning the spectral channels, the blue band shows roughly higher values than the other bands. If we reject this channel because of its worst fit, we obtain that in dense vegetated surfaces the spectral variability of the half width within its confidence interval is typically about 0.4º, without observing any regular spectral tendency. The spectral variability is not expected from the shading theory and it could be associated to the inversion procedure rather than to a physical process. The soil and corn samples show spectral differences up to 1º. In these cases, the hot spot half width decreases with the wavelength as opposed to the trend predicted by the coherent backscatter mechanism (Hapke, 1993). Although both mechanisms can occur in the same medium, it is expected that one dominate the formation of the hot spot. In addition, at longer wavelengths (>700 nm), the increasing multiple scattered radiance may favor the coherent mechanism (Hapke et al. 1996). Further investigations are required to explain this spectral dependence and determine if the coherent backscattering contribute to the enhancement of reflectance at backscatter, especially in the NIR region.

Figure 4 shows the retrieved amplitude. Unlike the half width, the amplitude presents a regular pattern regarding the canopy cover type. The spectral variability is also consistent with the expected reflectance of leaves and soil particles. Photosynthetically active vegetated samples (alfalfa, wheat, legumes) show higher amplitude in the green channel than in the blue and red ones, showing the highest values for the NIR. In contrast, non-photosynthetically active samples (soil and barley) show wavelength scaled amplitude according to the optical properties of the dry leaves. The derived amplitude is higher in the afternoon flight than at noon, in agreement with the theoretical formulation considered above (eq. 3). The variability within the classes is slightly higher than it could be expected from the nadir reflectance values. This could be partly associated to the errors introduced in the inversion procedure. Finally, the lowest amplitude values at 443 nm indicate the low aerosol contribution to the hot spot (Breón et al. 2002).

Finally, the leaf reflectance of the samples was estimated using the equation 3. This equation is valid for thick canopies, i.e. when the soil contribution is negligible. Therefore, the soil and corn (~25% cover)

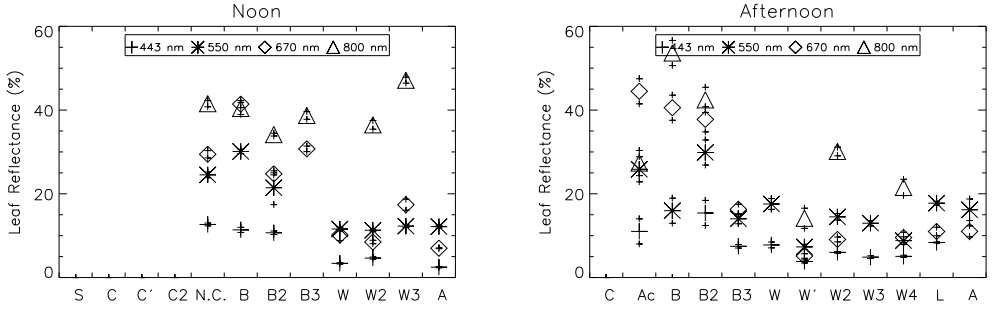

Figure 5. Leaf reflectance estimation in the noon and afternoon flights.

targets have been not considered. Results can be observed in figure 5. In general, the results are satisfactory when using the more confident data (noon flight). The estimated spectral leaf reflectance shows coherent results. For example, barley presents increasing reflectance values with the wavelength as expected from its senescent stage, whereas green vegetated samples show high values at 550 nm than at 670 nm. In the noon flight, we can observe certain variability in samples corresponding to a same canopy type, e.g. samples B and B2, because of the differences in amplitude previously reported (see figure 2a and 2c). The afternoon flights present worse results mainly associated to the directional under-sampling. This result in an underestimation of NIR reflectance for the wheat samples.

5. CONCLUSION

In this paper, we have analyzed the hot spot directional signatures of different vegetation covers derived from POLDER airborne data acquired during DAISEX'99 campaign. The retrieval of the hot spot directional signatures relies on the assumption of spatial homogeneity of the target. The data points of the hot spot signature have been fitted to a function of the phase angle (eq 3). The amplitude and the half-width of the measured hot spot have been retrieved using the method proposed by Bréon et al. 2002.

The half width ranged between 1º-2º independently of the canopy cover type. This reveals the difficulty to infer structural information of the canopies from the half width. Some samples (soil, corn, barley) have shown an unexpected spectral dependence of the hot spot half width. Further investigations should be desirable to explain this result.

The retrieved values of the amplitude of hot spot and the leaf reflectance are consistent with the expectations, providing thus information linked with the phenological status of the canopy.

Nevertheless, the retrieved parameters are quite sensitive to the distribution of data points along the hot spot geometry. In fact, the hot spot domain is roughly 5 degrees in phase angle. Consequently, and because the noise in the data, a poor sampling of this domain will translate into biased estimates of the hot spot parameters. In this way, the amplitude seems to be underestimated and the half-width overestimated when the hot spot peak is undersampled. Complementary measures of the hot spot from HyMAP data taken during this campaign will be used to analyze both the influence of the sampling in the hot spot domain and the spectral dependence in the half-width.

ACKNOWLEDGEMENTS

This work has been partially supported by the 'Scientific Analysis of the ESA Airborne Multi-Annual Imaging Spectrometer Campaign DAISEX' project. Special thanks are due to Dr. F.M. Bréon for his contribution to this work.

REFERENCES

Barabanenkov, Y.N., Y.A. Kravtsov, V.D. Ozrin and A.I. Saichev, 1991, Enhanced backscattering in optics, In Progress in Optics, vol. 29 (E. Wolf, Ed.), Elsevier, New York, pp. 65-197.

Bréon, F.M., F. Maignan, M. Leroy and I. Grant, 2002, Analysis of the hot spot directional signatures measured from space, Journal of Geophysical Research, 107, D16, 10.1029-10.1044

Bréon, F.M., V. Vanderbilt, M. Leroy, P. Bicheron, C.L. Walthall and J.E. Kalshoven, 1997, Evidence of hot spot directional signatures from airborne POLDER measurements, IEEE Transactions on Geoscience and Remote Sensing, 35, 2, 479-484.

ESA, 2001, Proceedings of the DAISEX final results workshop, ESA SP-499, ESA Publication Division, ESTEC, The Netherlands, July 2001 (277 pp).

García-Haro, F.J, Sommer, S. and Kemper, T. (2002), Variable multiple endmember spectral mixture analysis (VMESMA): a high performance computing and environment analysis tool, *Remote Sensing of Environment*, in revision.

Hapke, B., D. Dimucci, R. Nelson and W. Smythe, 1996, The cause of the hot spot in vegetation canopies and soils: shadow-hiding versus coherent backscatter. Remote Sensing of Environment, 58, 63-68.

Hapke, B., 1993, Topics in remote sensing 3: Theory of Reflectance and Emittance Spectroscopy, Cambridge University Press. 455 pp.

Jupp, D.L.B. and A.H. Strahler, 1991, A hotspot model for leaf canopies, Remote Sensing of Environment, 38, 193-210.

Kuusk, A., 1985, The hot spot effect of a uniform vegetative cover, Soviet Journal of Remote Sensing, 3, 645-658.

Leroy, M, O. Hatecoeur, F. Ponchaut, L. Alonso-Chorda, and J. Moreno, 2001, The airborne POLDER data in the DAISEX'99 campaign, ESA SP-499, ESA Publication Division, ESTEC, The Netherlands, July 2001, 13-22.

Qin,W. and N.S.Goel, 1995, An evaluation hotspot models for vegetation canopies, Remote Sensing Reviews, 13,121-159.

Roujean, J.L., 2000, A parametric hot spot model for optical remote sensing application, Remote Sensing of Environment, 71: 197-206.

Seeliger, H., 1887, Zur theorie der Beleuchtung der grossen planeten inbesondere des Saturn, Abhandl. Bayer. Akad. Wiss. Math-Naturw. Kl. II 16: 405-516.